

QUT Digital Repository:  
<http://eprints.qut.edu.au/>



Frost, Ray L. and Cejka, Jiri (2009) *A Raman spectroscopic study of the uranyl mineral rutherfordine – revisited*. *Journal of Raman Spectroscopy*, 40(9). pp. 1096-1103.

© Copyright 2009 John Wiley and Sons

1 **A Raman spectroscopic study of the uranyl mineral rutherfordine – revisited**

2  
3 **Ray L. Frost<sup>1</sup> • and Jiří Čejka<sup>1,2</sup>**

4  
5 <sup>1</sup> Inorganic Materials Research Program, School of Physical and Chemical  
6 Sciences, Queensland University of Technology, GPO Box 2434, Brisbane  
7 Queensland 4001, Australia.

8  
9 <sup>2</sup> National Museum, Václavské náměstí 68, CZ-115 79 Praha 1, Czech Republic.

10  
11 **The molecular structure of the uranyl mineral rutherfordine has been**  
12 **investigated by the measurement of the NIR and Raman spectra and**  
13 **complemented with infrared spectra including their interpretation. The**  
14 **spectra of the rutherfordine show the presence of both water and**  
15 **hydroxyl units in the structure as evidenced by IR bands at 3562 and 3465**  
16 **cm<sup>-1</sup> (OH) and 3343, 3185 and 2980 cm<sup>-1</sup> (H<sub>2</sub>O). Raman spectra show the**  
17 **presence of four sharp bands at 3511, 3460, 3329 and 3151 cm<sup>-1</sup>.**  
18 **Corresponding molecular water bending vibrations were only observed in**  
19 **both Raman and infrared spectra of one of two studied rutherfordine**  
20 **samples. The second rutherfordine sample studied contained only**  
21 **hydroxyl ions in the equatorial uranyl plane and did not contain any**  
22 **molecular water. The infrared spectra of the (CO<sub>3</sub>)<sup>2-</sup> units in the**  
23 **antisymmetric stretching region show complexity with three sets of**  
24 **carbonate bands observed. This combined with the observation of**  
25 **multiple bands in the (CO<sub>3</sub>)<sup>2-</sup> bending region in both the Raman and IR**  
26 **spectra suggests that both monodentate and bidentate (CO<sub>3</sub>)<sup>2-</sup> units may**  
27 **be present in the structure. This cannot be exactly proved and inferred**  
28 **from the spectra; however, it is in accordance with the X-ray**  
29 **crystallographic studies. Complexity is also observed in the IR spectra of**  
30 **(UO<sub>2</sub>)<sup>2+</sup> antisymmetric stretching region and is attributed to non-identical**  
31 **UO bonds. U-O bond lengths were calculated using wavenumbers of the**  
32  **$\nu_3$  and  $\nu_1$  (UO<sub>2</sub>)<sup>2+</sup> and compared with data from X-ray single crystal**

---

• Author to whom correspondence should be addressed (r.frost@qut.edu.au)

33 **structure analysis of rutherfordine. Existence of solid solution having a**  
34 **general formula  $(\text{UO}_2)(\text{CO}_3)_{1-x}(\text{OH})_{2x}\cdot y\text{H}_2\text{O}$  ( $x, y \geq 0$ ) is supported in the**  
35 **crystal structure of rutherfordine samples studied.**

36

37

38 **KEYWORDS:** rutherfordine, uranyl carbonate, molecular water, hydroxyls, infrared  
39 and Raman spectroscopy, U-O and O-H...O bond lengths

---

40

41

42

43

## 44 INTRODUCTION

45

46 Uranyl carbonate solid state and solution chemistry plays one of the most  
47 important roles in the actinide chemistry, mineralogy, geochemistry and  
48 environmental chemistry with regards to uranium(VI) migration and to spent nuclear  
49 fuel problems <sup>1,2</sup>. Uranyl carbonates and their soluble complexes are also important in  
50 uranium mining and technology and are found in the oxidation zone as products of  
51 uraninite hydration-oxidation weathering in the form of uranyl minerals <sup>3</sup>. Known  
52 uranyl carbonate minerals may be divided in several groups: the most frequent uranyl  
53 tricarbonates (such as andersonite, bayleyite, liebigite), tetracarbonates (fontanite),  
54 dicarbonates (zellerite), hydroxocarbonates (rabbittite, sharpite) and monocarbonates  
55 (rutherfordine, blatonite and joliotite). Some uranyl carbonates contain other anions  
56 (schroekinggerite, albrechtschraufite, lepersonnite) <sup>4</sup>.

57

58 All known analyzed samples of orthorhombic uranyl carbonate rutherfordine,  
59  $a = 4.840(1)$ ,  $b = 9.273(2)$ ,  $c = 4.298(1)$  Å,  $Z = 2$ , space group  $C^{20}_{2v} = Imm2$  <sup>5</sup> contain  
60 small amounts of OH groupings in the form of molecular water and/or hydroxyl ions.  
61 Frondel <sup>6</sup> writes that this small amount of water may be essential to the structure of  
62 rutherfordine. Smith <sup>3</sup> assumes that variable amounts of water can enter the interlayer  
63 region of the layered structure of rutherfordine. This may lead up to the formation of  
64 blatonite or joliotite. OH groupings were found also in a set of synthetic analogues of  
65 rutherfordine and related synthetic phases <sup>7,8</sup> [and many references therein]. However  
66 no structural relation between rutherfordine, blatonite and joliotite was observed.  
67 Christ *et al.* <sup>9</sup> showed the structure consists of sheets of  $(CO_3)^{2-}$  groups lying parallel  
68 in a plane perpendicular to the  $b$  axis, with linear  $(UO_2)^{2+}$  groups inserted into  
69 hexagonal holes normal to the sheets. A stacking disorder is present, involving the  
70 choice of parallel or antiparallel orientation of  $(CO_3)^{2-}$  groups in adjacent sheets <sup>9</sup>.  
71 Finch *et al.* refined the structure of rutherfordine <sup>5</sup>. Finch showed that  $(CO_3)^{2-}$  groups  
72 in alternate layers have the same orientation, not opposite orientations as originally  
73 reported by Christ *et al.* <sup>9,10</sup>. Topology of uranyl layers arrangement in rutherfordine  
74 was discussed by Burns <sup>4,11</sup>.

75

76 The infrared spectra of rutherfordine and its synthetic analogues has been  
77 published <sup>12</sup>. Interpretation of the infrared spectra of rutherfordine somewhat differs in

78 the papers cited. As mentioned above, some of the natural and synthetic rutherfordine  
79 samples studied contained various amounts of water. This corresponds with Frondel<sup>6</sup>  
80 who writes that all the rutherfordine samples show a small amounts of water  
81 contained on heating above 110° C, which may be essential to the structure.  
82 Composition of rutherfordine and its synthetic analogues may be therefore somewhat  
83 variable. Composition of synthetic  $(\text{UO}_2)(\text{CO}_3)_{1-x}(\text{OH})_{2x} \cdot n\text{H}_2\text{O}$  proves that no  
84 adsorbed water is present in such phases but some solid solutions with limited  
85 solubility of  $\text{UO}_2(\text{OH})_2 \cdot x\text{H}_2\text{O}$  in  $\text{UO}_2\text{CO}_3$  may exist. Raman spectrum of rutherfordine  
86 was given without any detailed interpretation by Wilkins<sup>13,14</sup> (only a graph and the  
87 wavenumber of the  $\nu_1(\text{UO}_2)^{2+}$  were published by Wilkins). Frost and Čejka also  
88 reported the Raman spectroscopic analysis of a rutherfordine sample<sup>15,16</sup> One of the  
89 difficulties in studying the infrared (and Raman) spectra of uranyl carbonates is the  
90 potential overlap of bands associated with  $(\text{UO}_2)^{2+}$  and the  $(\text{CO}_3)^{2-}$  units. The region  
91 for the symmetric stretching vibration of the  $(\text{CO}_3)^{2-}$  units is a spectral window free  
92 from bands ascribed to the  $(\text{UO}_2)^{2+}$  units. One potential overlap is between the  
93 antisymmetric stretching vibrations of the  $(\text{CO}_3)^{2-}$  units and the  $\delta$  bending water  
94 modes. Another major difficulty is the possible overlap of the symmetric stretching  
95 modes of the  $(\text{UO}_2)^{2+}$  units and the bending modes of the  $(\text{CO}_3)^{2-}$  units. There is  
96 another consideration caused by the presence or absence of water in the structure.  
97 The presence of water may cause significant shifts in the bands associated with both  
98  $(\text{UO}_2)^{2+}$  units and  $(\text{CO}_3)^{2-}$  units.

99

100 Čejka made tentative assignments of the bands for rutherfordine as follows:  $\nu_3$   
101 of  $(\text{UO}_2)_{2+}$  at  $985\text{ cm}^{-1}$ ,  $\nu_1$  not observed in the infrared,  $\nu_2$  in the  $255$  to  $260\text{ cm}^{-1}$  range  
102<sup>7,8</sup>. It is apparent that the application of Raman spectroscopy can assist with the  
103 assignation of these bands. According to Čejka and Urbanec the  $(\text{CO}_3)^{2-}$  ion symmetry  
104 is lowered from  $D_{3h}$  to  $C_{2v}$ <sup>7,8</sup>. The assignation of the  $(\text{CO}_3)^{2-}$  bands was given as  $\nu_1$  at  
105  $1112\text{ cm}^{-1}$ ,  $\nu_2$  at  $804\text{ cm}^{-1}$ ,  $\nu_3$  at  $1415$  and  $1503\text{ cm}^{-1}$  and  $\nu_4$  at around  $702$  and  $781\text{ cm}^{-1}$   
106<sup>12</sup>. This is in agreement and comparable with calculated data for  $\text{UO}_2\text{CO}_3$   $1110$ ,  $807$ ,  
107  $1520$  and  $1433$ ,  $707$  and  $783\text{ cm}^{-1}$ , respectively. Some variation in band position  
108 between different measurements is noted. According to Čejka<sup>12</sup>, the splitting of the  $\nu_3$   
109 bands cannot be used to ascertain whether the carbonates are bidentate or  
110 monodentate. X-ray crystallography studies by Christ et al and Finch *et al.* indicate  
111 that both mono and bidentate structures exist in the natural mineral<sup>5,9</sup>.

112

113 Urbanec and Čejka also suggest that rutherfordine is not a non-hydrated, non-  
114 hydroxylated carbonate as infrared bands were observed in the 3000 to 3600  $\text{cm}^{-1}$   
115 region<sup>17,18</sup>. Čejka and Urbanec suggested that solid-solutions with limited solubility  
116 may exist in the system  $\text{UO}_2\text{CO}_3\text{-UO}_2(\text{OH})_2\cdot x\text{H}_2\text{O}$ , thus forming  $\text{UO}_2(\text{CO}_3)_{1-x}$   
117  $(\text{OH})_{2x}\cdot y\text{H}_2\text{O}$ . This assumption was later discussed and accepted by Finch *et al.*<sup>5</sup> and  
118 Catalano and Brown<sup>19</sup>. It is assumed that this type of substitution could occur in the  
119 structure if  $\text{U}^{6+}$  coordination polyhedra adjacent to a missing  $(\text{CO}_3)$  group distorted  
120 from hexagonal dipyramids to pentagonal dipyramids. Such a distortion would  
121 probably shift the U atoms only slightly, as for the topologically similar mineral  
122 schmitterite<sup>20</sup>. According to Catalano and Brown<sup>19</sup>, the rutherfordine sample studied  
123 by EXAFS may contain more water and/or hydroxyls that could hydrogen bond to  
124  $\text{O}_{\text{axial}}$ , increasing its bond valence and extending the U- $\text{O}_{\text{axial}}$  distance. This supports  
125 the conclusions reached by Čejka and Urbanec<sup>8,17,21</sup>. Composition of a set of  
126 synthetic  $\text{UO}_2(\text{CO}_3)_{1-x}(\text{OH})_{2x}\cdot y\text{H}_2\text{O}$  ( $x, y \geq 0$ ) prepared under different conditions  
127 proves that practically no adsorbed water is present in such phases and some solid  
128 solutions with limited solubility of  $\text{UO}_2(\text{OH})_2\cdot x\text{H}_2\text{O}$  in  $\text{UO}_2\text{CO}_3$  may exist. Čejka and  
129 Urbanec inferred on the basis of interpretation of infrared spectra and thermal analysis  
130 a more ordered layered (polymeric) structure of hydrothermally synthesized uranyl  
131 monocarbonate phases ( $\nu_3(\text{UO}_2)^{2+}$  970  $\Rightarrow$  986  $\text{cm}^{-1}$ ) and a „disordered“ layered  
132 structure of uranyl monocarbonate phases prepared at laboratory temperature ( $\nu_3$   
133  $(\text{UO}_2)^{2+}$  approximately 956-965  $\text{cm}^{-1}$ ). Natural uranyl carbonate rutherfordine ( $\nu_3$   
134  $(\text{UO}_2)^{2+}$  ~ 985  $\text{cm}^{-1}$ ) corresponds to those of synthetic uranyl carbonate prepared  
135 under hydrothermal conditions<sup>8,17,21</sup>. Theoretical study of bonding in  $\text{UO}_2\text{CO}_3$  and  
136 its hydrated complexes was recently published<sup>22,23</sup>. New data on enthalpy of  
137 formation of rutherfordine,  $\text{UO}_2\text{CO}_3$ , were recently given by Kubatko *et al.*<sup>24</sup>.

138

139 In this work we attribute bands at various wavenumbers to vibrational modes  
140 of rutherfordine using Raman spectroscopy complemented with NIR and infrared  
141 spectroscopy.

142

143

144

145

146

147

## 148 **EXPERIMENTAL**

### 149 **Minerals**

150

151 The rutherfordine minerals used in this work were obtained from Museum  
152 Victoria.

153

### 154 **Raman microprobe spectroscopy**

155

156 The crystals of rutherfordine were placed and orientated on the stage of an  
157 Olympus BHSM microscope, equipped with 10x and 50x objectives and part of a  
158 Renishaw 1000 Raman microscope system, which also includes a monochromator, a  
159 filter system and a Charge Coupled Device (CCD). Raman spectra were excited by a  
160 HeNe laser (633 nm) at a resolution of  $2\text{ cm}^{-1}$  in the range between 100 and 4000  
161  $\text{cm}^{-1}$ . Repeated acquisition using the highest magnification was accumulated to  
162 improve the signal to noise ratio. Spectra were calibrated using the  $520.5\text{ cm}^{-1}$  line of  
163 a silicon wafer. Details of the technique have been published by the authors<sup>25-28</sup>.

164

165

### 166 **Infrared Spectroscopy**

167

168 Infrared spectra were obtained using a Nicolet Nexus 870 FTIR spectrometer  
169 with a smart endurance single bounce diamond ATR cell. Spectra over the 4000–525  
170  $\text{cm}^{-1}$  range were obtained by the co-addition of 64 scans with a resolution of  $4\text{ cm}^{-1}$   
171 and a mirror velocity of  $0.6329\text{ cm/s}$ .

172

173 Spectral manipulation such as baseline adjustment, smoothing and  
174 normalisation was performed using the GRAMS® software package (Galactic  
175 Industries Corporation, Salem, NH, USA).

176

177 **Near-infrared (NIR) spectroscopy**

178

179 NIR spectra were collected on a Nicolet Nexus FT-IR spectrometer with a  
180 Nicolet Near-IR Fibreport accessory (Madison, Wisconsin). A white light source was  
181 used, with a quartz beam splitter and TEC NIR InGaAs detector. Spectra were  
182 obtained from 13 000 to 4000  $\text{cm}^{-1}$  (0.77-2.50  $\mu\text{m}$ ) by the co-addition of 64 scans at a  
183 spectral resolution of 8  $\text{cm}^{-1}$ . A mirror velocity of 1.266  $\text{m sec}^{-1}$  was used. The  
184 spectra were transformed using the Kubelka-Munk algorithm to provide spectra for  
185 comparison with published absorption spectra. Spectral manipulations, such as  
186 baseline correction, smoothing and normalisation, were performed using the software  
187 package GRAMS (Galactic Industries Corporation, NH, USA).

188

189 **RESULTS AND DISCUSSION**

190

191 **Near-infrared spectroscopy**

192

193 NIR spectroscopy has proven most useful for the study of minerals<sup>38-43</sup>. The  
194 technique can identify the presence of both water and OH units in the mineral  
195 structure. The near-infrared spectra may be conveniently divided into sections  
196 according to the attribution of bands in this spectral region. Accordingly spectra are  
197 divided into (a) the spectral region between 4000 and 8000  $\text{cm}^{-1}$ ; this region is  
198 corresponds to the first fundamental overtone of the mid-infrared OH stretching  
199 vibration, together with the water OH overtones and carbonate combination bands  
200 and (b) the spectral region between 8000 and 12000  $\text{cm}^{-1}$ ; this region corresponds to  
201 the second fundamental overtone of the OH stretching vibrations and also includes  
202 electronic bands resulting from transition metal ions in the structure<sup>29-37</sup>. Two NIR  
203 bands at 9900 and 11110  $\text{cm}^{-1}$  are attributed to these electronic bands.

204

205 The NIR spectrum of rutherfordine in the 6500 to 12000  $\text{cm}^{-1}$  region is shown  
206 in *Fig. 1*. Mierjerink showed that the position of the higher energy states can be  
207 obtained from the UV-Vis absorption spectrum<sup>44</sup>. This band is associated with  
208 electronic transitions and is the region of the second fundamental overtone of the OH  
209 stretching vibrations. These OH stretching vibrations will be composed of two

210 components resulting from the overtones of the OH units and the water vibrations.  
211 However the intensity of the electronic band will significantly override the latter.  
212 Three component bands are observed at 8575, 9900 and 11110  $\text{cm}^{-1}$ . The broad bands  
213 are attributed to the  $\text{UO}_2^{2+}$  ion electronic transitions. This band contributes to the  
214 colour of uranyl containing minerals<sup>45</sup>. The information in this spectral region reveals  
215 the oxidation states of uranium and can fundamentally be used to fingerprint minerals  
216 containing uranium<sup>46,47</sup>. The absorption properties of  $\text{U}^{4+}$  and  $\text{U}^{6+}$  are well known<sup>45</sup>.  
217 The principal absorption bands of  $\text{U}^{4+}$  are in the 22,000 to 8000  $\text{cm}^{-1}$  region. The  
218  $\text{UO}_2^{2+}$  unit absorbs below 22,000  $\text{cm}^{-1}$ . Most uranium minerals absorb in the UV-  
219 Visible region as well as the NIR. In NIR spectra bands have been reported for  
220 selected uranium minerals at around 14,000  $\text{cm}^{-1}$  and broad bands for meta-autunite  
221 and uranophane at this position were assigned to the  $\text{UO}_2^{2+}$  units<sup>45</sup>. No further detail  
222 of the absorption bands such as the electronic transitions were made.

223

224 Three NIR bands are observed at 6885, 6960 and 7520  $\text{cm}^{-1}$ . These bands  
225 result from the first fundamental overtone of the OH stretching vibrations. Thus NIR  
226 spectroscopy proves the existence of OH and/or water units in the rutherfordine  
227 structure. Bands at 8575 and 9000  $\text{cm}^{-1}$  are assigned to the overtones of the stretching  
228 vibrations of water. It must be considered that all combinations of bands are allowed.  
229 Thus the possibility of bands can arise from the following combinations (a)  $2\nu_1$  (IR)  
230 (b)  $2\nu_1$  (Raman) (c)  $2\nu_3$  (IR) and (d)  $2\nu_3$  (Raman). The combination of Raman and  
231 infrared bands is also allowed. Thus bands may also arise from ( $\nu_1$ (IR) +  $\nu_1$  (Raman))  
232 and other combinations. Thus although the spectral profile as shown shows three  
233 component bands it is probable that all the combinations delineated above are  
234 contained in this spectral profile.

235

236

237 The NIR spectrum in the 4000 to 6500  $\text{cm}^{-1}$  region is reported in *Fig. 2*  
238 (supplementary information). Two spectral regions are observed (a) the region around  
239 6000  $\text{cm}^{-1}$  and the region around 5000  $\text{cm}^{-1}$ . The three NIR bands at 5705, 5890 and  
240 6060  $\text{cm}^{-1}$  are attributed to the overtone of the combination bands of the carbonate  
241 anion of rutherfordine. The bands arise from  $2(\nu_1 + \nu_3)$  of the carbonate anion.

242

243

## 244 Raman Spectroscopy

245

246 The Raman and infrared spectra of the 1000 to 1700  $\text{cm}^{-1}$  region are shown in  
247 Figs. 3 and 4. The Raman spectrum shows a single intense band at 1115  $\text{cm}^{-1}$  with a  
248 bandwidth of 3.4  $\text{cm}^{-1}$ . The band is attributed to the  $\nu_1$  symmetric stretching mode of  
249 the  $(\text{CO}_3)^{2-}$  units. In the infrared spectrum (*Fig. 4*) a low intensity band is observed at  
250 1110  $\text{cm}^{-1}$  which is also assigned to this vibration. From a theoretical point of view  
251 for a carbonate anion of perfect symmetry, this band should be Raman active-infrared  
252 inactive. Thus the observation of the band in the infrared spectrum suggests some loss  
253 of symmetry. This value agrees well with the published result of Urbanec and Čejka  
254 who found a value of 1112  $\text{cm}^{-1}$  <sup>17</sup>. Theoretical calculations suggest a value of 1110  
255  $\text{cm}^{-1}$  <sup>12</sup>.

256

257 In the Raman spectrum an intense band is observed at 1412  $\text{cm}^{-1}$  with a  
258 shoulder at 1381  $\text{cm}^{-1}$ . These bands are assigned to the  $(\text{CO}_3)^{2-}$   $\nu_3$  antisymmetric  
259 stretching vibrations. The infrared spectrum in the 1250 to 1700  $\text{cm}^{-1}$  region is  
260 complex with a complex series of overlapping bands. A set of bands are observed at  
261 1333, 1366 and 1414,  $\text{cm}^{-1}$ . A second set of bands is found at 1505 and 1544  $\text{cm}^{-1}$ .  
262 These bands are assigned to the  $\nu_3$  antisymmetric stretching vibrations of  $(\text{CO}_3)^{2-}$   
263 units. This splitting of the  $\nu_3$  modes of  $(\text{CO}_3)^{2-}$  units has been observed by Čejka <sup>12</sup>.  
264 However the complexity of the infrared spectral profile has not been observed in the  
265 Raman spectrum. X-ray diffraction studies have shown the existence of both mono  
266 and bidentate carbonate ions. X-ray diffraction determines lattice structures whereas  
267 infrared spectroscopy determines molecular structures. The complexity of the infrared  
268 spectral profile in the  $(\text{CO}_3)^{2-}$  antisymmetric stretching region seems to indicate  
269 multiple species of carbonate anions in the rutherfordine structure. The splitting of the  
270  $\nu_3$   $(\text{CO}_3)^{2-}$  vibrations suggests that monodentate and bidentate carbonate groups may  
271 be together present in the crystal structure of rutherfordine <sup>48</sup>. However, any detailed  
272 resolution of mono- and bidentate carbonate ligands from the infrared and Raman  
273 spectra is not possible in the structure of rutherfordine. Bands in the infrared spectrum  
274 of rutherfordine sample studied in this region are 1544, 1505, 1414, 1366, 1333, 1110  
275  $\text{cm}^{-1}$ .

276

277

278 The Raman and infrared spectrum of rutherfordine in the 600 to 1000 cm<sup>-1</sup>  
 279 region are shown in *Figs. 5* and *6* respectively. An intense band is observed in the  
 280 Raman spectrum at 866 cm<sup>-1</sup>. This band is assigned to the  $\nu_1$  symmetric stretching  
 281 mode of the (UO<sub>2</sub>)<sup>2+</sup> units. U-O bond lengths in uranyl were calculated with empirical  
 282 relations by Bartlett and Cooney<sup>49</sup>. In the infrared spectrum the profile is complex  
 283 and as with the antisymmetric stretching region of (CO<sub>3</sub>)<sup>2-</sup> units so with the  
 284 antisymmetric stretching region of the uranyl units, multiple bands are observed.  
 285 Band component analysis shows bands at 866, 921, 956 and 982 cm<sup>-1</sup>. It is probable  
 286 that the bands at 921, 956 and 982 cm<sup>-1</sup> are attributed to the (UO<sub>2</sub>)<sup>2+</sup>  $\nu_3$  antisymmetric  
 287 stretching and bands at 779 and 804 to the  $\nu_1$  symmetric stretching vibrations of  
 288 (UO<sub>2</sub>)<sup>2+</sup> units, respectively. The positions of the bands are in agreement with  
 289 published data<sup>12</sup>. No bands were observed in the positions 900-970 cm<sup>-1</sup> in the  
 290 Raman spectra. Bands at 866 and 921 cm<sup>-1</sup> may be connected with the UO<sub>2</sub>O<sub>6</sub> uranyl  
 291 hexagonal dipyramidal coordination polyhedra with four carbonate groups in the  
 292 uranyl equatorial plane, while that at 956 cm<sup>-1</sup> which may be attributed to the  $\delta$  U-OH  
 293 bending vibration, probably with the UO<sub>2</sub>O<sub>5</sub> uranyl pentagonal dipyramidal  
 294 coordination polyhedra with some (OH)<sup>-</sup> groups in the uranyl equatorial plane.  
 295 According to Čejka and Urbanec, the higher is the carbon dioxide pressure in  
 296 rutherfordine formation, the higher is the wavenumber of the  $\nu_3$  (UO<sub>2</sub>)<sup>2+</sup> and the lower  
 297 is the U-O bond length in uranyl in the crystal structure of rutherfordine. Empirical  
 298 relations by Bartlett and Cooney<sup>49</sup>  
 299 ( $R_{U-O} = 0.804 + 91.41(\nu_3)^{-2/3}$  and  $R_{U-O} = 0.575 + 106.5(\nu_1)^{-2/3}$ ) and by Čejka<sup>12a</sup> ( $R_{U-O}$   
 300  $= 1.0882 + 65.356(\nu_3)^{-2/3}$ ) were used.. Calculated U-O bond lengths in uranyl are: IR  
 301  $\nu_3$  (UO<sub>2</sub>)<sup>2+</sup> Å/cm<sup>-1</sup>): 1.724/1.746/991; 1.729/1.749/983; 1.737/1.755/970;  
 302 1.752/1.766/947; IR  $\nu_1$  (UO<sub>2</sub>)<sup>2+</sup>, 1.732/883; 1.755/857; Raman  $\nu_1$  (UO<sub>2</sub>)<sup>2+</sup> 1.730/885;  
 303 1.738/876. U-O bond length inferred from single crystal structure analysis of  
 304 rutherfordine is 1.744(8) Å<sup>5</sup>, from EXAFS analysis 1.77 Å<sup>50</sup> and 1.764(2) Å and  
 305 from infrared spectrum 1.745 Å<sup>51</sup>. Average U-O bond lengths (in uranyl) are 1.779 Å  
 306 in schoepite and 1.777<sub>6</sub> Å in metaschoepite. Wavenumber at 947 cm<sup>-1</sup>, which may be  
 307 related to  $\delta$  U-OH bending vibration and UO<sub>2</sub>O<sub>5</sub> coordination polyhedron in the  
 308 crystal structure of studied rutherfordine sample, corresponds to U-O bond length  
 309 1.752 Å. According to the X-ray single crystal structure analysis<sup>5</sup>, there are only one  
 310 symmetrically distinct U<sup>6+</sup>/ [UO<sub>2</sub>O<sub>6</sub>] and one symmetrically distinct C<sup>4+</sup>/ [CO<sub>3</sub>]

311 present in rutherfordine, however, this is not in full agreement with data observed and  
312 inferred from the Raman and infrared spectroscopy. Infrared spectrum of the second  
313 studied sample of rutherfordine shows absorption bands at  $982\text{ cm}^{-1}$ , attributed to the  
314  $\nu_3(\text{UO}_2)^{2+}$  antisymmetric stretching vibration, at  $921\text{ cm}^{-1}$ , connected with the  $\nu_1$   
315  $(\text{UO}_2)^{2+}$  symmetric stretching vibration, and at  $956\text{ cm}^{-1}$ , assigned to the  $\delta$  U-OH  
316 bending vibration. Calculated U-O bond lengths in uranyl are ( $\nu_3$ )  $1.729\text{ \AA}$  and  $1.750$   
317  $\text{\AA}$ , and ( $\nu_1$ )  $1.700\text{ \AA}$ .

318

319 An intense Raman band is observed at  $838\text{ cm}^{-1}$  with two other bands at  $787$   
320 and  $821\text{ cm}^{-1}$  (Fig. 5). It is suggested that the band at  $838\text{ cm}^{-1}$  is attributable to the  $\nu_2$   
321 bending modes of the  $(\text{CO}_3)^{2-}$  units and that the two bands of lesser intensity at  $799$   
322 and  $784\text{ cm}^{-1}$  are due to the  $\nu_4$  out of plane bending modes. In the  $77\text{ K}$  Raman  
323 spectrum, two bands are observed at  $839$  and  $833\text{ cm}^{-1}$ . These bands are ascribed to  
324 the  $\nu_2$  bending modes. In the infrared spectrum two bands are observed at  $784$  and  
325  $804\text{ cm}^{-1}$  and are assigned to this mode (Fig. 6). Čejka observed infrared bands at  
326  $804$  or  $806\text{ cm}^{-1}$ <sup>12</sup>. In the  $77\text{ K}$  Raman spectrum two bands are observed at  $799$  and  
327  $786\text{ cm}^{-1}$ . The likely assignment of these bands is to the  $\nu_4$  bending modes of the  
328  $(\text{CO}_3)^{2-}$  units. In the infrared spectrum bands are found at  $757$ ,  $779$ ,  $784\text{ cm}^{-1}$  and  $701$   
329  $\text{cm}^{-1}$ . These bands are assigned to the  $\nu_4$  bending modes of the  $(\text{CO}_3)^{2-}$  units. Only a  
330 very low intensity infrared band is observed in the  $298\text{ K}$  Raman spectrum at  $701\text{ cm}^{-1}$   
331 <sup>1</sup>. The multiple bands in the  $\nu_4$  bending region indicate (a) a lowering of symmetry  
332 and (b) multiple  $(\text{CO}_3)^{2-}$  units. Infrared bands of the second rutherfordine sample  
333 studied observed in this region are  $701$ ,  $757$ ,  $779$ ,  $784$  and  $804\text{ cm}^{-1}$ .

334

335 The low wavenumber region of rutherfordine is shown in Fig. 7. In the  
336 Raman spectrum, bands are observed at  $401$ ,  $433$ ,  $458$ ,  $513$  and  $547\text{ cm}^{-1}$ . The  $458$   
337  $\text{cm}^{-1}$  band in the  $298\text{ K}$  spectrum splits into four bands at  $403$ ,  $438$ ,  $463$ ,  $477\text{ cm}^{-1}$  in  
338 the  $77$  spectrum (Fig. not shown). The  $343\text{ cm}^{-1}$  band seems to split into two  
339 components at  $336$  and  $330\text{ cm}^{-1}$ . These bands may be attributed to the  $\nu$  (U-O<sub>ligand</sub>)  
340 vibrations<sup>52</sup>. The bands at  $279$ ,  $263$ ,  $252$  and  $241\text{ cm}^{-1}$  may be ascribed to the  $\nu_2$   
341 bending modes of the  $(\text{UO}_2)^{2+}$  units. Some of these bands may be assigned to the  
342 lattice vibrations.

343

344 The Raman spectrum in the 2500 to 3600  $\text{cm}^{-1}$  region of rutherfordine is  
345 shown in *Fig. 8*. Three bands are observed in the 298 K Raman spectrum at 3192,  
346 3279 and 3396  $\text{cm}^{-1}$ . The infrared spectrum of rutherfordine (*Fig. 9*) shows a broad  
347 profile with component bands at 2936 and 3316  $\text{cm}^{-1}$ . Other bands are observed at  
348 2345, 2364, 2531 and 2637  $\text{cm}^{-1}$ . The two sharp bands at 2345 and 2364  $\text{cm}^{-1}$  may be  
349 assigned to  $(\text{CO}_3)^{2-}$  overtones of the fundamental vibrations. Urbanec and Čejka  
350 suggested that broad bands were found in the infrared spectrum of some samples of  
351 rutherfordine<sup>53</sup>. They attributed these bands to water or hydroxyl units hydrogen  
352 bonded in the rutherfordine structure. In the structural reports for rutherfordine no  
353 water or hydroxyl units were identified. Raman complimented with infrared  
354 spectroscopy brings into question the variability of the rutherfordine structure. The  
355 presence of low intensity bands assigned to the hydroxyl deformation modes in the  
356 infrared spectrum at around 1635  $\text{cm}^{-1}$  supports the concept of water and/or hydroxyl  
357 units incorporation into the rutherfordine structure and probable existence of solid  
358 state solutions with limited solubility of the  $\text{UO}_2(\text{OH})_2 \cdot x\text{H}_2\text{O}$  in  $\text{UO}_2\text{CO}_3$ , as proved  
359 by Čejka and Urbanec<sup>17,21</sup>. Incorporation of OH groupings and hydrogen bonding  
360 cause a lowering of the wavenumber of the  $\nu_3(\text{UO}_2)^{2+}$  and elongation of the U-O  
361 bond length in uranyl. This may be one of the reasons, why synthetic hydrothermal  
362 uranyl carbonate phases prove the relatively shortest U-O bond lengths and the  
363 highest values of the wavenumber of the  $\nu_3(\text{UO}_2)^{2+}$  in comparison with those  
364 prepared under laboratory temperature and low pressure of carbon dioxide. U-O bond  
365 lengths in natural rutherfordine are more related to those of hydrothermal synthetic  
366 phases. The presence of a set of hydrogen bonds approximately varying in the range  
367 2.65 to 3.05 Å may be inferred from the wavenumbers of the  $\nu$  OH stretching  
368 vibrations observed<sup>54</sup>. Infrared bands of the second rutherfordine sample studied in  
369 this region are 3310  $\text{cm}^{-1}$  (2.76 Å) and 2930  $\text{cm}^{-1}$  (2.64) attributed to the  $\nu$  OH  
370 stretching vibration of hydrogen bonded hydroxyls, while bands observed at 2630 and  
371 2530 may be connected with combination bands and/or overtones and sharp bands at  
372 2360 and 2340  $\text{cm}^{-1}$  probably with carbon dioxide from the air. The second  
373 rutherfordine sample does not contain any molecular water, because no band was  
374 observed close to 1600  $\text{cm}^{-1}$  which could be attributed to the  $\delta$   $\text{H}_2\text{O}$  bending vibration.  
375  
376

377 **CONCLUSIONS**

378

379 Rutherfordine is an interesting mineral as the vibrational spectroscopy  
380 supports the concept of water and/or hydroxyl units being incorporated into the  
381 mineral structure thus forming solid solutions with limited solubility of  
382  $\text{UO}_2(\text{OH})_{2 \cdot x}\text{H}_2\text{O}$  (schoepite, metaschoepite, and dehydrated schoepite) in theoretically  
383 anhydrous uranyl carbonate  $\text{UO}_2\text{CO}_3$ . Hydroxyls may be present in the uranyl  
384 carbonate layers together with interstitial water molecules all participating in the  
385 formed hydrogen bonding network. Partial transformation of  $\text{UO}_2\text{O}_6$  hexagonal  
386 dipyramidal coordination polyhedra into  $\text{UO}_2\text{O}_5$  pentagonal dipyramidal polyhedra  
387 caused by partial  $(\text{CO}_3)^{2-} \Leftrightarrow 2 (\text{OH})^-$  substitution is assumed<sup>5,7</sup>. Bands attributed to the  
388  $\delta$  U-OH bending vibrations are also observed in the spectrum of rutherfordine.  
389 Raman spectroscopy at 298 and 77 K together with infrared spectroscopy has been  
390 used to assist in the elucidation of the rutherfordine mineral structure.  
391 Theoretically may exist anhydrous uranyl carbonate  $\text{UO}_2\text{CO}_3$  – rutherfordine,  
392 however, in fact practically all studied rutherfordine samples contain small amounts  
393 of molecular water and/or hydroxyl ions and may be understood as partly altered  
394  $\text{UO}_2\text{CO}_3$  thus forming solid solutions  $\text{UO}_2(\text{CO}_3)_{1-x}(\text{OH})_{2x} \cdot y\text{H}_2\text{O}$  in the system  
395 rutherfordine-schoepite or metaschoepite or dehydrated schoepite, where x and y are  
396 close to zero. Crystal structures of such natural phases are close to theoretically  
397 anhydrous rutherfordine  $\text{UO}_2\text{CO}_3$ <sup>5</sup>.

398

399 This work serves to show the application of Raman spectroscopy for the in-  
400 situ analysis of a uranyl carbonate mineral known as rutherfordine. The use of the  
401 microscope and associated Raman spectrometer allows single crystals are selected for  
402 the analysis. It should be noted there is almost no sample preparation apart from the  
403 alignment of the crystals in the incident beam. Raman spectroscopy may be used with  
404 a thermal stage allowing spectra to be obtained at any temperature. The collection of  
405 Raman data at liquid nitrogen temperature enables significantly improved band  
406 separation. Raman spectroscopy has by its very nature normally narrow bands as  
407 compared with infrared spectroscopy, and by obtaining data at 77 K, improved signal  
408 to noise is achieved.

409

410 **Acknowledgements**

411

412           The financial and infra-structure support of the Queensland University of  
413 Technology Inorganic Materials Research Program of the School of Physical and  
414 Chemical Sciences is gratefully acknowledged. The Australian Research Council  
415 (ARC) is thanked for funding. Mr Dermot Henry of Museum Victoria is thanked for  
416 the supply of the rutherfordine mineral.

417

418

419

420

421

422

423

424

425

426 **REFERENCES**

427

- 428 1. Clark, DL, Hobart, DE, Neu, MP. *Chem. Rev.* 1995; **95**.
- 429 2. McClaine, LA, Bullwinkel, EP, Huggins, JC. "Proc. 1st Intern. Conf. Peaceful  
430 Uses At. Energy 26 Geneva 1955".
- 431 3. Smith, DK *Uranium mineralogy*: Institution of Mining and Metallurgy,  
432 London 1984.
- 433 4. Anthony, JW, Bideaux, RA, Bladh, KW, Nichols, MC *Handbook of*  
434 *Mineralogy*; Mineral Data Publishing: Tuscon, Arizona, USA, 2003; Vol. 5.
- 435 5. Finch, RJ, Cooper, MA, Hawthorne, FC, Ewing, RC. *Can. Min.* 1999; **37**:  
436 929.
- 437 6. Frondel, C, Meyrowitz, R. *Am. Min.* 1956; **41**: 127.
- 438 7. Cejka, J. *Sb. Vysoke Skoly Chem.-Technol. Praze, Mineral.* 1965; **7**: 75.
- 439 8. Cejka, J, Urbanec, Z. *Coll. Czechoslovak Chem. Com.* 1973; **38**: 2327.
- 440 9. Christ, CL, Clark, JR, Evans, HT, Jr. *Science* 1955; **121**: 472.
- 441 10. Clark, JR, Christ, CL. *Am. Min.* 1956; **41**: 844.
- 442 11. Burns, PC, Finch, R, Editors *Uranium: Mineralogy, Geochemistry and the*  
443 *Environment. (Proceedings of a Short Course held 22-23 October 1999 in*  
444 *Golden, Colorado.) [In: Rev. Mineral., 1999; 38], 1999.*
- 445 12. Cejka, J. *Rev. Min.* 1999; **38**: 521.
- 446 13. Wilkins, RWT. *Neues Jahr. Min.* 1971: 440.
- 447 14. Wilkins, RWT. *Z. Kristallogr., Kristallgeometrie, Kristallphys., Kristallchem.*  
448 1971; **134**: 285.
- 449 15. Frost, RL, Cejka, J. *J. Raman Spectrosc.* 2007; **38**: 1488.
- 450 16. Weier, ML, Frost, RL, Reddy, BJ. *J. Near Infrared Spec.* 2005; **13**: 359.
- 451 17. Urbanec, Z, Cejka, J. *Collection of Czechoslovak Chemical Communications*  
452 1979; **44**: 1.
- 453 18. Urbanec, Z, Čejka, J. "Thermal Analysis Vol. 1"; Proc. 4th Int. Conf. Thermal  
454 Analysis, Budapest
- 455 19. Catalano, JG, Brown, GE, Jr. *Am. Min.* 2004; **89**: 1004.
- 456 20. Meinrath, G. *J. Radioanal. Nucl. Chem.* 1996; **211**: 349.
- 457 21. Urbanec, Z, Cejka, J. *Casopis Narodniho Muzea v Praze, Rada Prirodovedna*  
458 1979; **148**: 16.
- 459 22. Majumdar, D, Balasubramania, K, Nitsche, H. *Chem. Phys. Lett.* 2002; **361**:  
460 143.
- 461 23. Majumdar, D, Roszak, S, Balasubraanian, KL, Nitsche, H. *Chem. Phys. Lett.*  
462 2003; **372**: 232.
- 463 24. Kubatko, KA, Helean, KB, Navrotsky, A, Burns, PC. *Am. Min.* 2005; **90**:  
464 1284.
- 465 25. Frost, RL, Weier, ML. *Thermochim. Act.* 2003; **406**: 221.
- 466 26. Frost, RL, Weier, ML, Klopogge, JT. *J. Raman Spectrosc.* 2003; **34**: 760.
- 467 27. Frost, RL, Weier, ML. *J. Raman Spectrosc.* 2003; **34**: 776.
- 468 28. Frost, RL, Weier, ML. *Thermochim. Act.* 2004; **409**: 79.
- 469 29. Frost, RL, Palmer, SJ, Reddy, BJ. *Vib. Spec.* 2007; **44**: 154.
- 470 30. Frost, RL, Reddy, BJ, Wain, DL, Martens, WN. *Spectrochim. Act.* 2007; **66**:  
471 1075.
- 472 31. Frost, RL, Wain, DL, Martens, WN, Reddy, BJ. *Spectrochim. Act.* 2007; **66A**:  
473 1068.
- 474 32. Palmer, S, Reddy, BJ, Frost, RL. *Polyhedron* 2007; **26**: 524.

- 475 33. Reddy, BJ, Frost, RL. *Spectrochim. Act.* 2007; **66A**: 312.
- 476 34. Reddy, BJ, Frost, RL. *J. Near Infrared Spec.* 2007; **15**: 115.
- 477 35. Reddy, BJ, Frost, RL, Martens, WN, Wain, DL, Kloprogge, JT. *Vib. Spec.*  
478 2007; **44**: 42.
- 479 36. Reddy, BJ, Frost, RL, Weier, ML, Martens, WN. *J. Near Infrared Spec.* 2006;  
480 **14**: 241.
- 481 37. Frost, RL, Wills, R-A, Martens, W, Weier, M, Reddy, BJ. *Spectrochim. Act.*  
482 2005; **62A**: 42.
- 483 38. Hunt, GR. *Geophys.* 1977; **42**: 501.
- 484 39. Hunt, GR, Ashley, RP. *Econ. Geol.* 1979; **74**: 1613.
- 485 40. Hunt, GR, Ashley, RP. Altered-rock spectra in the visible and near infrared; U.  
486 S. Geol. Surv., Denver, CO, USA., 1979; pp. 57 pp.
- 487 41. Hunt, GR, Hall, RB. *Clays Clay Min.* 1981; **29**: 76.
- 488 42. Hunt, GR, Salisbury, JW. *Mod. Geol.* 1970; **1**: 283.
- 489 43. Hunt, GR, Salisbury, JW, Lenhoff, CJ. *Mod. Geol.* 1973; **4**: 85.
- 490 44. Meijerink, A. *Lum. Sol.* 1998: 45.
- 491 45. Hanchar, JM. *Rev. Min.* 1999; **38**: 499.
- 492 46. Benard, P, Louer, D, Dacheux, N, Brandel, V, Genet, M. *Chem. Mat.* 1994; **6**:  
493 1049.
- 494 47. Haberlandt, H, Hernegger, F, Scheminsky, F. *Spectrochim. Act.* 1950; **4**: 21.
- 495 48. Jolivet, JP, Thomas, Y, (, BT. *J. Mol. Struct.* 1980; **60**: 93.
- 496 49. Bartlett, JR, Cooney, RP. *J. Mol. Struct.* 1989; **193**: 295.
- 497 50. Thompson, HA, Brown, GE, Jr., Parks, GA. *Physica* 1995; **208 & 209**: 167.
- 498 51. Sejkora, J, Cejka, J, Hlousek, J, Novak, M, Srein, V. *Can. Min.* 2004; **42**: 963.
- 499 52. Hoekstra, HR, Siegel, S. *J. Inorg. Nuc. Chem.* 1973; **35**: 761.
- 500 53. Cejka, J, Urbanec, Z. *Casopis Narodniho Muzea v Praze, Rada Prirodovedna*  
501 1979; **146**: 114.
- 502 54. Libowitzky, E. *Monat. Chem.* 1999; **130**: 1047.
- 503
- 504
- 505
- 506
- 507
- 508
- 509
- 510
- 511

*List of Figs.*

512

513

514 **Fig. 1** NIR spectrum of the 6500 to 12000  $\text{cm}^{-1}$  region of rutherfordine

515

516 **Fig. 2** NIR spectrum of the 4000 to 6500  $\text{cm}^{-1}$  region of rutherfordine

517

518 **Fig. 3** Raman spectrum of the 1000 to 1700  $\text{cm}^{-1}$  region of rutherfordine.

519

520 **Fig. 4** Infrared spectra of the 1100 to 1700  $\text{cm}^{-1}$  region of rutherfordine.

521

522 **Fig. 5** Raman spectra of the 600 to 1000  $\text{cm}^{-1}$  region of rutherfordine.

523

524 **Fig. 6** Infrared spectra of the 700 to 1000  $\text{cm}^{-1}$  region of rutherfordine.

525

526 **Fig. 7** Raman spectra of the 100 to 600  $\text{cm}^{-1}$  region of rutherfordine.

527

528 **Fig. 8** Raman spectra of the 2800 to 3600  $\text{cm}^{-1}$  region of rutherfordine.

529

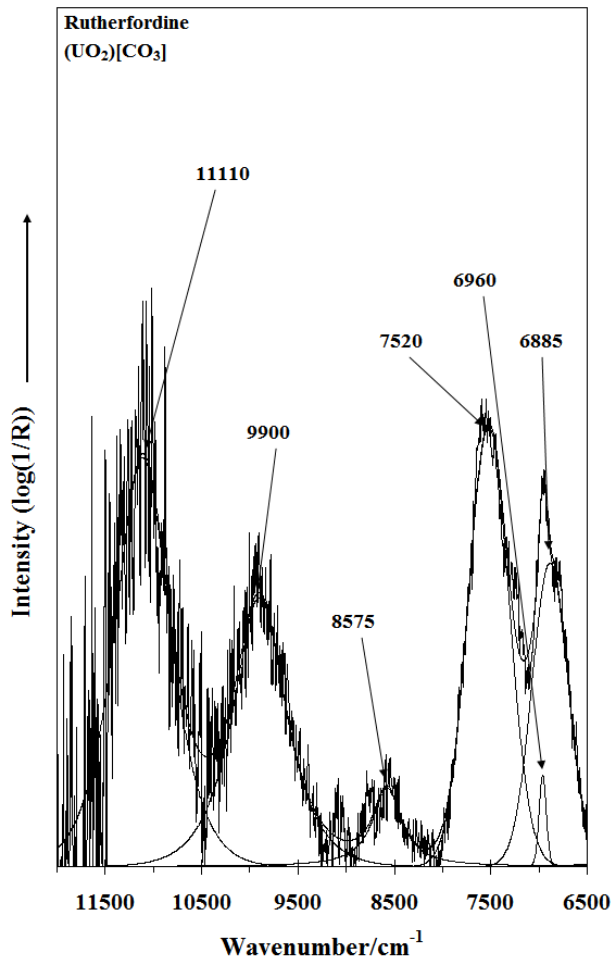
530 **Fig. 9** Infrared spectra of the 2200 to 3700  $\text{cm}^{-1}$  region of rutherfordine.

531

532

533

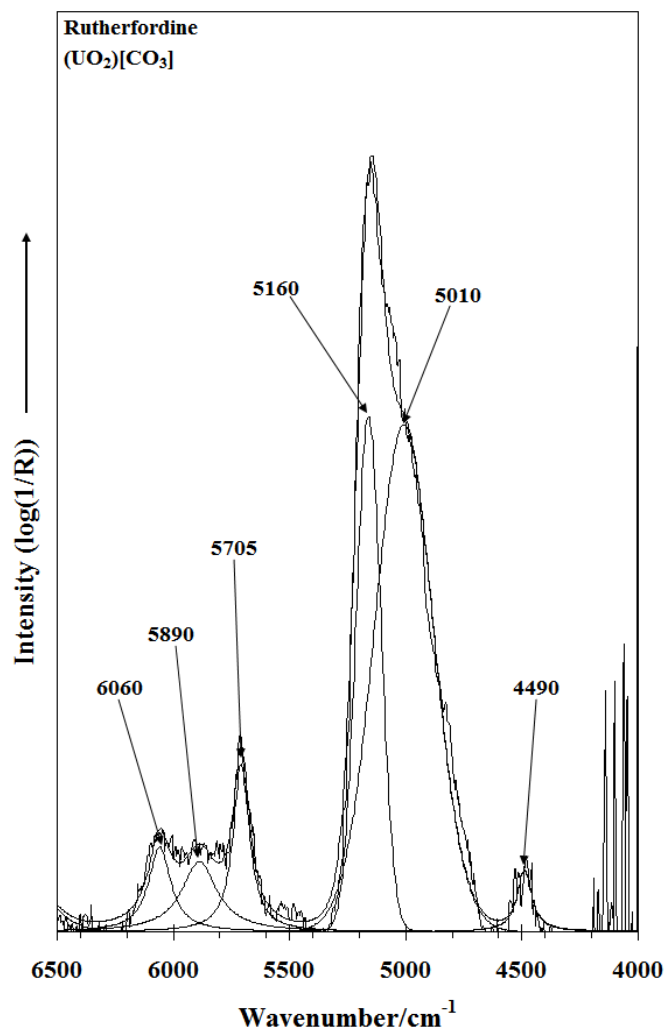
534



535

536

537 *Fig. 1*

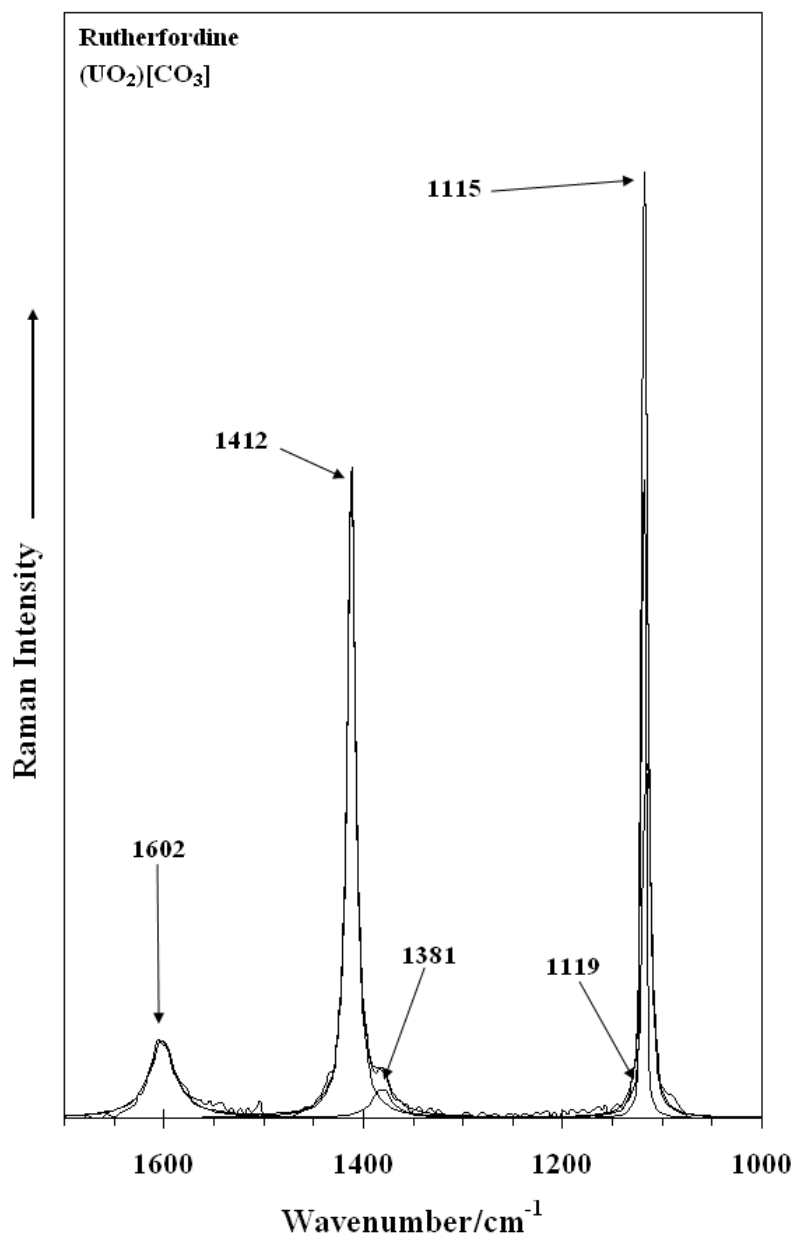


538

539

540 *Fig. 2*

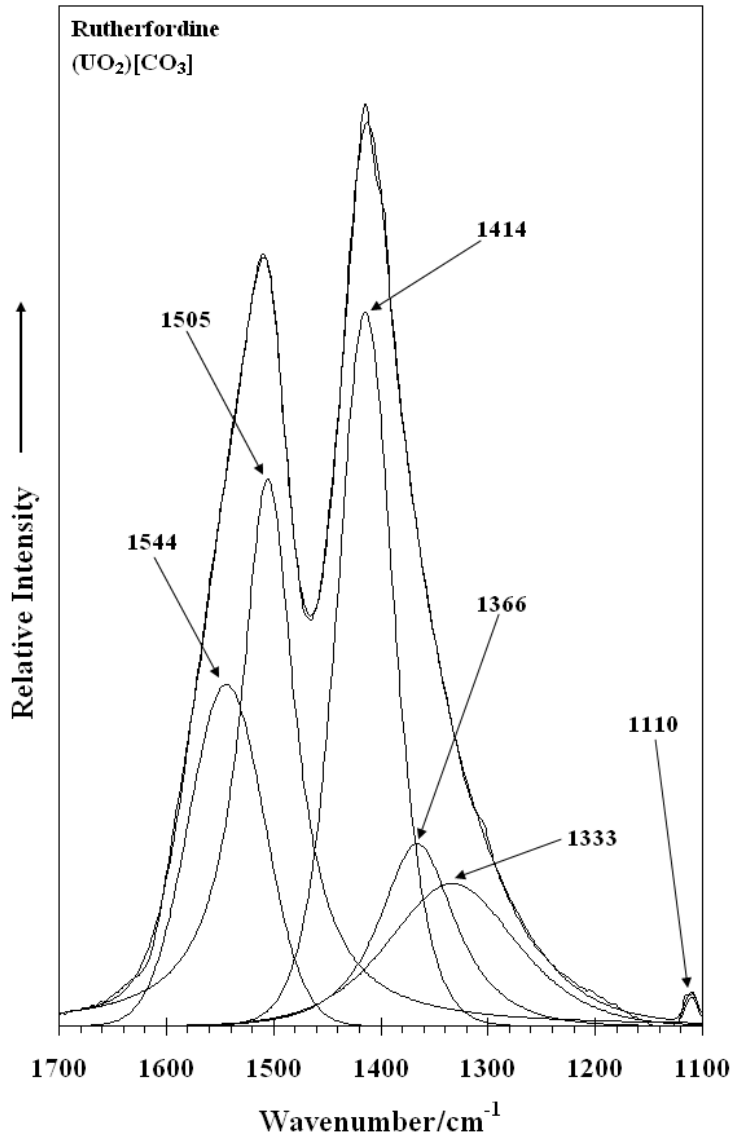
541



542

543 *Fig. 3*

544

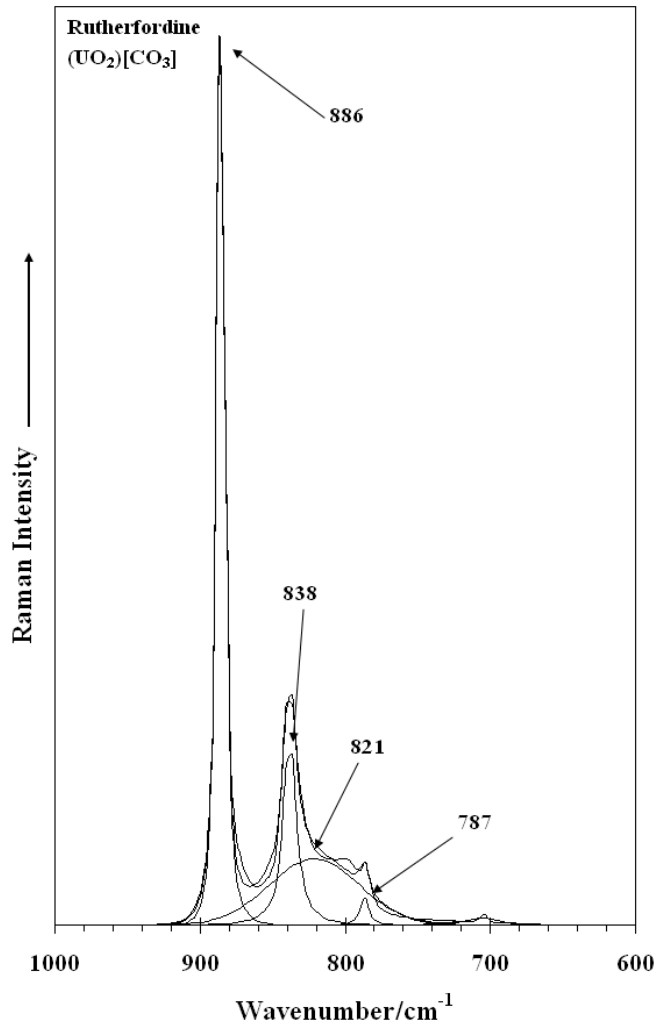


545

546 *Fig. 4*

547

548

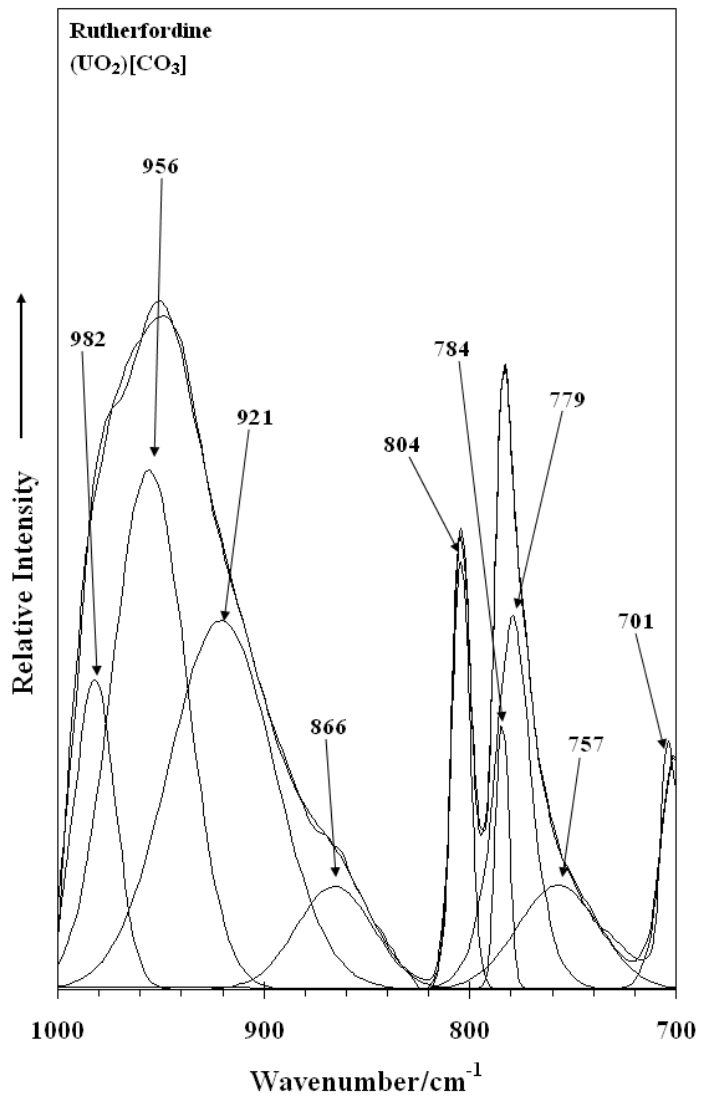


549

550 *Fig. 5*

551

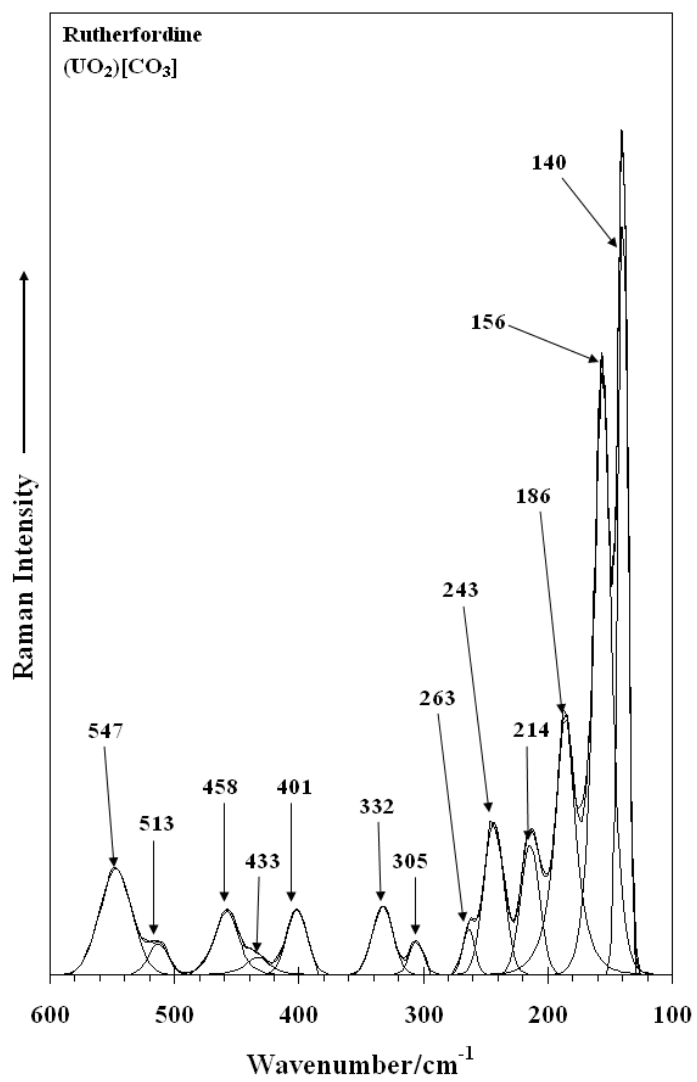
552



553

554

555 *Fig. 6*

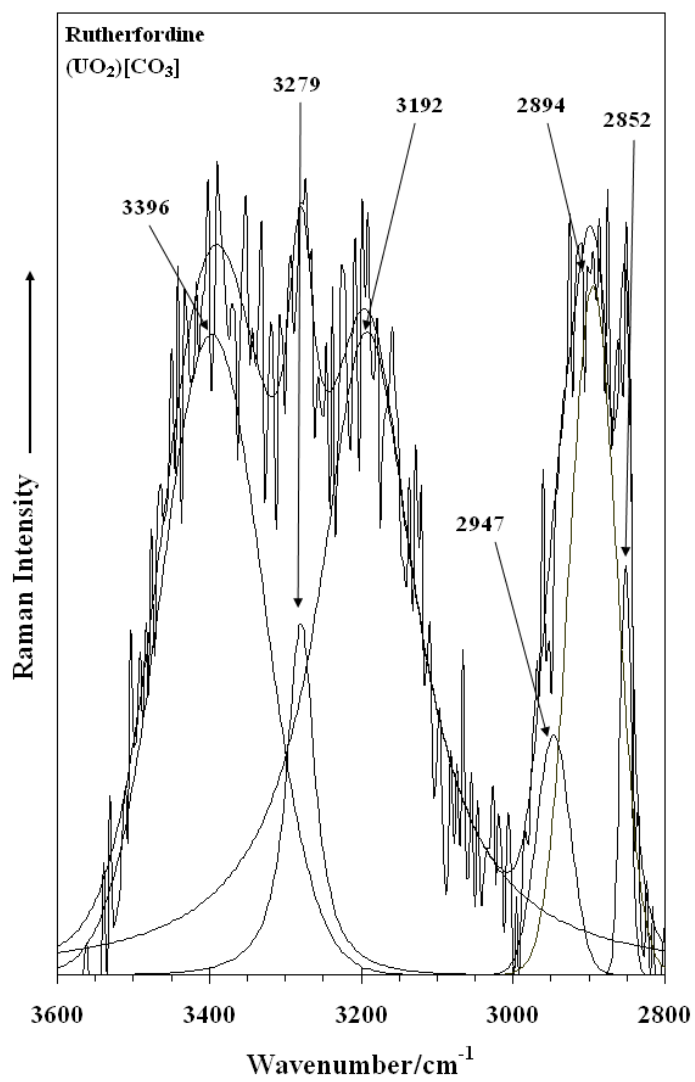


556

557

558 *Fig. 7*

559

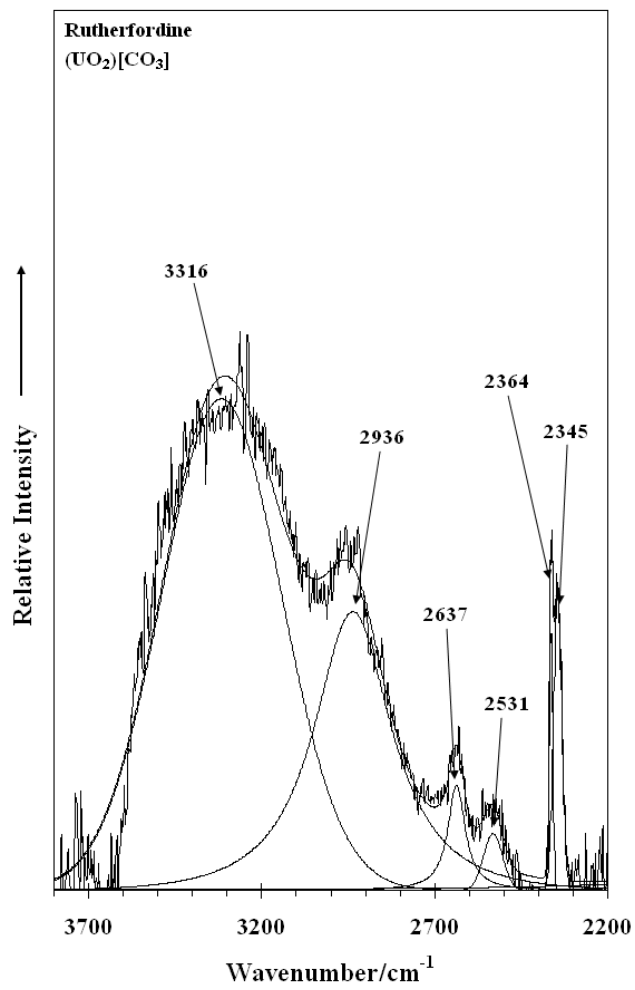


560

561 *Fig. 8*

562

563



564

565

566 **Fig. 9**

567